

Cite this article as: Du Yunling, Yang Yanhong, Zhou Yizhou. Optimal Duration Selection of Solid Solution Heat Treatment of Ni-based Single Crystal Superalloys Based on Statistical Analysis[J]. Rare Metal Materials and Engineering, 2022, 51(09): 3133-3137.

LETTER

# Optimal Duration Selection of Solid Solution Heat Treatment of Ni-based Single Crystal Superalloys Based on Statistical Analysis

Du Yunling<sup>1,2</sup>, Yang Yanhong<sup>1</sup>, Zhou Yizhou<sup>1</sup>

<sup>1</sup> Shi Changxu Innovation Center for Advanced Materials, Institute of Metal Research, Chinese Academy of Sciences, Shenyang 110016, China; <sup>2</sup> School of Materials Science and Engineering, University of Science and Technology of China, Shenyang 110016, China

**Abstract:** A novel approach was developed to select the optimal duration for solid solution heat treatment of Ni-based single-crystal (SX) superalloys based on the statistical analysis of  $\gamma'$  phase size in the second-generation SX superalloys. The microstructure uniformity  $\omega$  was introduced through the statistical analysis. The  $\omega$  curves can be divided into three stages according to the statistical analysis: the significant change area, transition area, and steady state area. The transition area shows the optimal duration range for solution heat treatment of Ni-based SX superalloys. This approach was verified by measuring the  $\gamma'$  rafting rate and testing the creep properties of alloys. Meanwhile, the accuracy of this approach was also validated through the fourth-generation Ni-based SX superalloys. This approach can effectively optimize the heat treatment and provide guidance for the design and engineering applications of SX superalloys.

**Key words:** Ni-based single-crystal superalloy; optimal duration of solution heat treatment;  $\gamma'$  rafting rate; creep property

Nickel-based single-crystal (SX) superalloys possess excellent mechanical properties and oxidation resistance at elevated temperatures, which have been widely used to manufacture the high/low-pressure turbine blades and vanes in advanced aircraft engines<sup>[1-3]</sup>. Their excellent mechanical properties derive from the unique  $\gamma/\gamma'$  two-phase microstructure in alloys, which is determined by the chemical composition, preparation technique, and particularly the heat treatment<sup>[1-8]</sup>. Usually, the heat treatments, such as the solution heat treatment (SHT) and aging heat treatment (AHT), have significant influence on the creep strength of alloys<sup>[7,9]</sup>. AHT can modify the morphology and volume fraction of  $\gamma'$  phase in alloys. SHT can eliminate the dendritic segregation and eutectic, but it is difficult to operate due to the complex and rapid microstructure evolution at high temperatures<sup>[10-15]</sup>. The maximum operating temperature of SHT is 5~10 °C lower than the initial melting temperature of Ni-based SX superalloys<sup>[15-17]</sup>, because the eutectic can quickly dissolve into  $\gamma$  matrix at the high temperature. Nevertheless, the optimal

SHT duration for homogeneous microstructure can hardly be decided. In fact, the solidification segregation cannot be completely eliminated during the actual SHT process of SX superalloys. Thus, the chemical composition and morphologies of the  $\gamma'$  phase between the interdendritic area and dendrite arm are slightly different<sup>[7,18-20]</sup>. Moreover, undesirable defects may be introduced during SHT. When the defects increase beyond the critical threshold, the mechanical properties of superalloys are significantly weakened. Therefore, SHT duration plays a key role in the preparation process of SX superalloys.

In this research, a novel approach was developed for the quantitative determination of SHT duration by evaluating the difference between  $\gamma'$  phase size in interdendritic area and that in dendrite arm area through statistical analysis.

## 1 Establishment of Statistical Analysis Model and Experiment

The microstructure uniformity ( $\omega$ ) is firstly introduced for

Received date: September 07, 2021

Foundation item: National Key R&D Program of China (2021YFB3700400); National Science and Technology Major Project (2017-VI-0003-0073)

Corresponding author: Yang Yanhong, Ph. D., Professor, Shi Changxu Innovation Center for Advanced Materials, Institute of Metal Research, Chinese Academy of Sciences, Shenyang 110016, P. R. China, Tel: 0086-24-23971807, E-mail: yhyang@imr.ac.cn

Copyright © 2022, Northwest Institute for Nonferrous Metal Research. Published by Science Press. All rights reserved.

the numerical analysis to characterize the difference in  $\gamma'$  precipitates in dendrite arm area and interdendritic area, as follows:

$$\omega = (L_{\gamma'_i} - L_{\gamma'_d}) / (L_{\gamma'_i} + L_{\gamma'_d}) \times 100\% \quad (1)$$

where  $L_{\gamma'_i}$  is the average size of  $\gamma'$  phase in interdendritic area and  $L_{\gamma'_d}$  is the average size of  $\gamma'$  phase in dendrite arm area. The  $\gamma'$  phase size is the averaged equivalent size. Then the  $\omega$  curves can be obtained based on statistical analysis of the  $\gamma'$  precipitates in dendrite arm and interdendritic areas after SHT for different durations. The  $\omega$  curve can be divided into three stages: significant change area, transition area, and steady state area. Afterwards, based on the tendency of  $\omega$  variation, the optimal range of  $\omega$  value is obtained. Correspondingly, the SHT duration can be effectively selected according to the optimal range of  $\omega$  value (transition area).

Long-term aging (LTA) and typical creep performance tests were conducted. Meanwhile, the approach accuracy was also verified through the fourth-generation Ni-based SX superalloys.

The nominal chemical composition of the second-generation Ni-based SX superalloy is listed in Table 1, and that of the fourth-generation Ni-based SX superalloy is reported in Ref.[21]. All specimens were machined along the [001] direction of SX bars prepared by the directional solidification method.

The heat treatments of the second- and fourth-generation SX superalloys are listed in Table 2. All the specimens underwent the air-cooling (AC) finally. SHT processes with different solution durations of 0, 2, 4, 8, and 16 h were conducted for S1~S5 specimens, respectively. Then these specimens underwent the same AHT process. Afterwards, S1~S5 specimens underwent the final LTA at 1100 °C for 0, 50, and 100 h. The fourth-generation SX superalloys after different heat treatments were named as F1~F5. The scanning electron microscope (SEM, TESCAN MIRA3) was used for microstructure observation after heat treatment and LTA. The

**Table 1 Nominal composition of Ni-based SX superalloy (wt%)**

Cr	Co	Al	Ti	Mo+Ta+W	Re	Hf	Ni
7.5	7.0	5.9	1.0	7.9	2.5	0.1	Bal.

**Table 2 Different heat treatments for the second- and fourth-generation SX superalloys**

Alloy	Specimen	Solid solution	Primary aging	Secondary aging
Second-generation SX superalloy	S1	1320 °C/0 h/AC (as-cast)		
	S2	1310 °C/2 h+1320 °C/2 h/AC		
	S3	1310 °C/2 h+1320 °C/4 h/AC	1080 °C/6 h/AC	900 °C/8 h/AC
	S4	1310 °C/2 h+1320 °C/8 h/AC		
	S5	1310 °C/2 h+1320 °C/16 h/AC		
Fourth-generation SX superalloy	F1	1315 °C/0 h/AC (as-cast)		
	F2	1315 °C/4 h+1325 °C /4 h/AC		
	F3	1315 °C/8 h+1325 °C/8 h/AC	1100 °C/4 h/AC	870 °C/24 h/AC
	F4	1315 °C/16h+1325 °C/16 h/AC		
	F5	1315 °C/24 h+1325 °C/24 h/AC		

specimens were mechanically polished and etched by the solution of 20 g CuSO<sub>4</sub>+100 mL HCl+5 mL H<sub>2</sub>SO<sub>4</sub>+80 mL H<sub>2</sub>O. The  $\gamma'$  phases were automatically identified and calculated by MIPAR software, and were characterized by red spots in Fig. 1a. The second- and fourth-generation SX alloys were machined into cylindrical specimens (diameter of 5 mm, gauge length of 25 mm) for tension creep tests at 1100 °C/120 MPa and 1140 °C/150 MPa, respectively.

## 2 Results and Discussion

SHT can mostly eliminate the composition segregation phenomenon. Since the morphology of  $\gamma'$  precipitates are closely related to the chemical composition, the microstructure uniformity  $\omega$  of  $\gamma'$  precipitates can be calculated to precisely evaluate the effect of segregation elimination. As shown in Fig. 1a, the uneven element diffusion rate between interdendritic area and dendrite arm area leads to different  $\gamma'$  phases. The statistical results of  $\gamma'$  sizes are summarized in Table 3, and the relationship between microstructure uniformity  $\omega$  with SHT duration is displayed in Fig. 1b. Clearly,  $\omega$  is decreased dramatically with slightly prolonging SHT duration, and this region is defined as the significant change area. With further prolonging the SHT duration,  $\omega$  is decreased mildly and enters a steady state. An obvious transition area between the significant change area and steady state area is obtained, which correspondingly refers to the optimal range of  $\omega$  ( $\omega_{op}$ ). Generally, the solidification segregation is still serious when  $\omega$  locates in the significant change area ( $\omega > \omega_{op}$ ). The homogenization and microstructure uniformity can hardly be further improved in the steady state stage. However, the undesirable defects including the homogenization pores are significantly increased.

Long-term SHT process is beneficial to the formation of uniform microstructure ( $\omega$  locates at the steady state area). Nevertheless, it is not suitable for engineering applications from the economic view. Therefore, the optimal SHT duration should be related to the transition area. LTA and creep tests were conducted for the second-generation SX superalloys.

The rafting behavior of  $\gamma'$  phase can be considered as the transition process from an unstable state to a stable state. This transition stems from the inhomogeneity of chemical

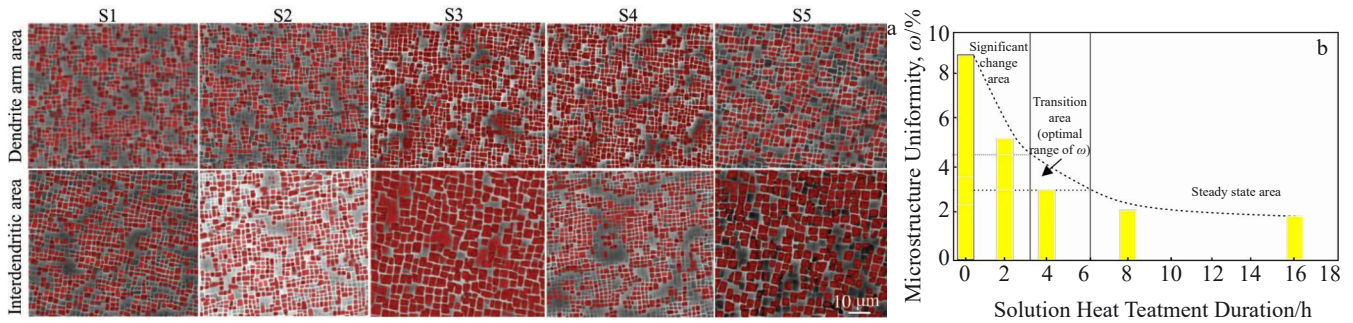


Fig.1 Microstructures of S1~S5 specimens in dendrite arm and interdendritic areas (a); relationship between microstructure uniformity  $\omega$  and SHT duration (b)

**Table 3**  $\gamma'$  sizes of interdendritic area and dendrite arm area in S1~S5 specimens after SHT and AHT processes ( $\mu\text{m}$ )

Area	S1	S2	S3	S4	S5
Interdendritic area	0.6856	0.3405	0.3645	0.3627	0.3365
Dendrite arm area	0.5781	0.3030	0.3383	0.3412	0.3201

composition in the dendritic arm and interdendrite areas. SHT can mostly eliminate the composition segregation, so the rafting difference of  $\gamma'$  phase between the dendrite arm and interdendritic areas ( $L_{\gamma'_i} - L_{\gamma'_d}$ ) can be used to evaluate the effect of different SHT processes. In order to obtain the more precise results, LTA process was interrupted when these specimens present a serious rafting phenomenon. Thus, LTA duration in this research is about 100 h. The statistical results of the  $\gamma'$  size in S1~S5 specimens after LTA at 1100 °C are shown in Fig. 2a. Accordingly, the rafting difference of  $\gamma'$  phase between dendrite arm and interdendritic ( $L_{\gamma'_i} - L_{\gamma'_d}$ ) can be calculated and shown in Fig.2b.

After aging for 50 and 100 h, the variation trends of  $L_{\gamma'_i} - L_{\gamma'_d}$  of S1~S5 specimens are similar to those without LAT. The transition area of these three curves appears in the similar region. When  $\omega > \omega_{op}$ , the rafting difference of S1 and S2 specimens is decreased rapidly. In addition, the rafting difference gradually reaches a stable state when  $\omega < \omega_{op}$ . Thus, it can be concluded that this statistical analysis method can obtain the optimal treatment duration for Ni-based SX superalloys.

The creep life of S1~S5 specimens is shown in Fig. 3. The creep life is initially increased with decreasing  $\omega$ , and it reaches the maximum value when SHT duration is 4 h ( $\omega$  locates in transition area). Afterwards, a dramatic drop can be observed. When  $\omega > \omega_{op}$ , the dendritic segregation cannot be effectively eliminated, leading to the short creep life of S1 and S2 specimens. When  $\omega < \omega_{op}$ , the dendritic segregation may be eliminated, and the chemical composition of the  $\gamma$  matrix and  $\gamma'$  precipitates in the dendrite arm and interdendritic areas becomes homogeneous. However, because the element diffusion is significant at elevated solution temperatures near the melting point, more undesirable defects, such as the homogenization pore (H-pore), are formed after SHT for longer duration (Fig. 3). These H-pores deform significantly

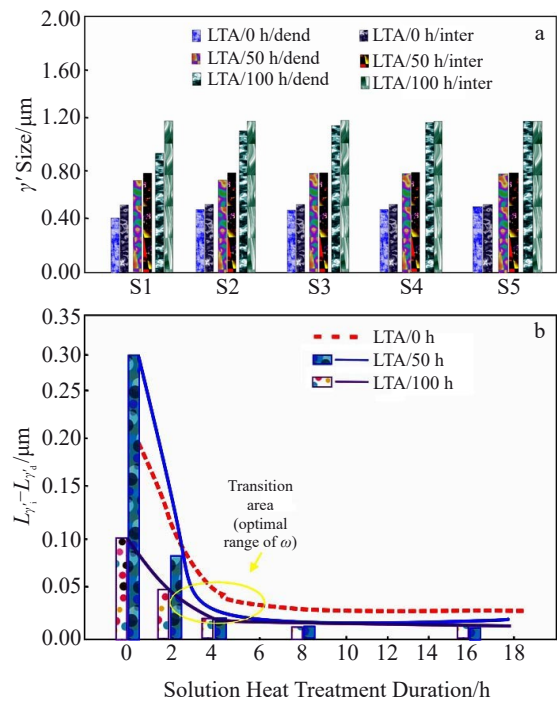


Fig.2  $\gamma'$  sizes of S1~S5 specimens after LTA at 1100 °C for different durations in different areas (a); rafting difference of  $\gamma'$  phase between dendrite arm and interdendritic areas (b) (dend and inter refer to dendritic arm area and interdendritic area, respectively)

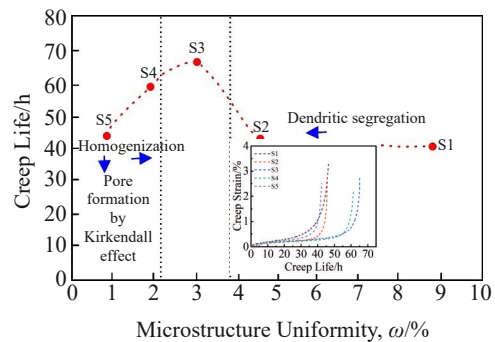


Fig.3 Relationship between creep life (1120 °C/120 MPa) and microstructure uniformity  $\omega$  of S1~S5 specimens

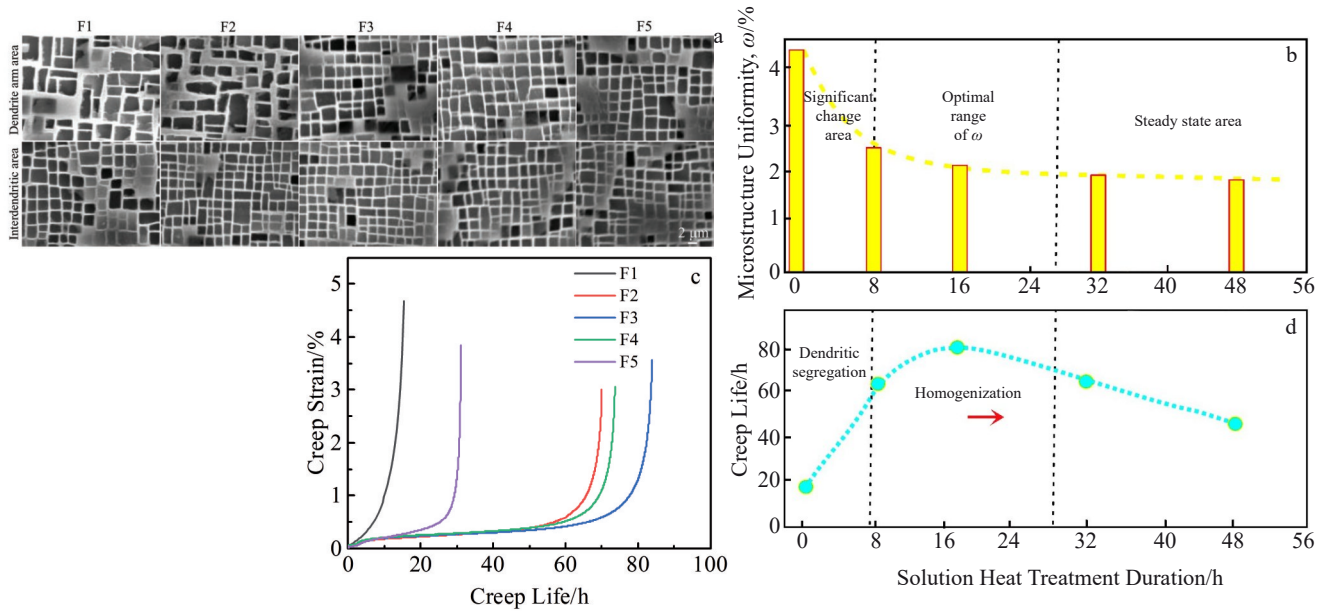


Fig.4 Microstructures of F1~F5 specimens in dendrite arm and interdendritic areas (a); relationship between microstructure uniformity  $\omega$  and SHT duration (b), relationship between creep strain (1140 °C/150 MPa) and creep life (c), relationship between creep life (1140 °C/150 MPa) and SHT duration (d) of F1~F5 fourth-generation SX superalloys

under the creep deformation and induce the initiation of microcrack. Therefore, the creep life is decreased. Besides, the creep strength can be improved when the optimal SHT duration is about 4 h ( $\omega$  locates in the optimal range). Hence, the accuracy of this statistical analysis approach for SHT duration selection is confirmed by creep test results.

The accuracy of the proposed approach is also validated by the fourth-generation Ni-based SX superalloys. As shown in Fig.4, the morphologies and distribution of  $\gamma'$  phase as well as the relationship between microstructure uniformity  $\omega$  and different SHT durations show the similar trends to those of the second-generation SX superalloys. In addition, the relationship between creep life and microstructure uniformity  $\omega$  of the fourth-generation Ni-based SX superalloys is also similar to that of the second-generation SX superalloys. The results in this research are consistent with those in Ref.[19].

### 3 Conclusions

1) The microstructure uniformity  $\omega$  can be obtained based on the relationship between creep performance and solution heat treatment duration.

2) The optimal duration selection of solid solution heat treatment of Ni-based single crystal superalloys based on statistical analysis shows accurate prediction, and it can provide guidance for investigation of other single crystal superalloys and the design of novel single crystal superalloys.

### References

- 1 Reed R C. *The Superalloys: Fundamentals and Applications*[M]. Cambridge: Cambridge University Press, 2006
- 2 Pollock T M, Argon A S. *Acta Metallurgica et Materialia*[J], 1992, 40(1): 1
- 3 Wu Y B, Ma X F, Zhang H Z et al. *Rare Metal Materials and Engineering*[J], 2016, 45(3): 588
- 4 Zhang J X, Ro Y, Zhou H et al. *Scripta Materialia*[J], 2006, 54(4): 655
- 5 Ratel N, Demé B, Bastie P et al. *Scripta Materialia*[J], 2008, 59(11): 1167
- 6 Wang X G, Liu J L, Jin T et al. *Scripta Materialia*[J], 2015, 99: 57
- 7 Zhang J X, Harada H, Koizumi Y. *Journal of Materials Research* [J], 2006, 21(3): 647
- 8 Xu T Z, Pan X H, Zhang M H et al. *Rare Metal Materials and Engineering*[J], 2021, 50(4): 1113
- 9 Hinchey E P, Barron D, Pomeroy M J et al. *Journal of Alloys and Compounds*[J], 2021, 857: 157 560
- 10 Yu J J, Sun X F, Zhao N R et al. *Materials Science and Engineering A*[J], 2007, 460-461: 420
- 11 Sponseller D L. *Superalloys*[M]. Warrendale: TMS, 1996: 256
- 12 Wasson A J, Fuchs G E. *Mater Charact*[J], 2012, 74: 11
- 13 Latief F H, Kakehi K, Murakami H. *Materials Science and Engineering A*[J], 2013, 567: 65
- 14 Wu E D, Sun G D, Chen B et al. *Acta Materialia*[J], 2013, 61(7): 2308
- 15 Fuchs G E. *Materials Science and Engineering A*[J], 2001, 300(1-2): 52
- 16 Horst O M, Adler D, Git P et al. *Materials and Design*[J], 2020, 195: 108 976
- 17 Ali M A, López-Galilea I, Gao S et al. *Materialia*[J], 2020, 12: 100 692

- 18 Zhang Y B, Liu L, Huang T W et al. *Scripta Materialia*[J], 2017, 136: 74
- 19 Trexler M D, Church B C, Sanders Jr T H. *Scripta Materialia*[J], 2006, 55(6): 561
- 20 Li P, Li S S, Han Y F. *Intermetallics*[J], 2011, 19(2): 182
- 21 Wang X G, Liu J L, Jin T et al. *Advanced Engineering Materials* [J], 2015, 17(7): 1034

## 基于统计分析的镍基单晶高温合金最佳固溶热处理时间选择

杜云玲<sup>1,2</sup>, 杨彦红<sup>1</sup>, 周亦霄<sup>1</sup>

(1. 中国科学院 金属研究所 师昌绪先进材料创新中心, 辽宁 沈阳 110016)

(2. 中国科学技术大学 材料科学与工程学院, 辽宁 沈阳 110016)

**摘要:** 提出了一种基于二代镍基单晶 (SX) 高温合金  $\gamma'$  相尺寸变化统计分析的 SX 高温合金固溶热处理最佳时间的选择方法。通过数值分析引入了微观结构均匀性  $\omega$ , 根据数据统计  $\omega$  曲线可分为 3 个阶段: 显著变化区、过渡区和稳态区。过渡区描述了固溶热处理时间选择的最佳范围。通过测量合金的  $\gamma'$  筏化和蠕变性能, 验证了该方法的有效性。同时也通过第四代镍基 SX 高温合金验证了该方法的准确性。该方法能够有效地建立最优的热处理工艺, 并为 SX 高温合金的设计和工程应用提供指导。

**关键词:** 镍基单晶高温合金; 最优热处理制度;  $\gamma'$  筏化; 蠕变性能

---

作者简介: 杜云玲, 女, 1986 年生, 博士生, 中国科学院金属研究所师昌绪先进材料创新中心, 辽宁 沈阳 110016, 电话: 024-23971083, E-mail: yldu18b@imr.ac.cn